

## Propagation of Drop Coalescence in a Two-Dimensional Emulsion: A Route towards Phase Inversion

Nicolas Bremond,\* Hugo Doméjean, and Jérôme Bibette

UPMC Université Paris 06, CNRS UMR 7195, ESPCI ParisTech, 10 rue Vauquelin, 75231 Paris, France

(Received 6 December 2010; published 24 May 2011)

The phase inversion that undergoes an emulsion while being sheared is a sudden phenomenon that is still puzzling. In this Letter, we report an experimental investigation on propagative coalescence by using a microfluidic device where a calibrated two-dimensional emulsion is created and destabilized. The velocity of propagation and the probability of the coalescence are reported as a function of the size and the spatial distribution of the drops, respectively. We then discuss the efficiency of this novel scenario of phase inversion and suggest that inversion can be favored by the existence of a drop size distribution.

DOI: 10.1103/PhysRevLett.106.214502

PACS numbers: 47.55.df, 47.57.Bc, 47.61.Jd

An emulsion is a metastable dispersion of one liquid into a second one in the presence of surface active agents. Two main physical mechanisms govern the destruction of such a system: One involves the diffusion of the dispersed phase through the continuous phase, namely, Ostwald ripening, and a second one concerns the coalescence of neighboring drops [1]. The destabilization of a concentrated emulsion under shear can lead to a phase inversion; i.e., the continuous phase becomes the dispersed phase and vice versa. This sudden transition can be induced by modifying the surfactant properties, by tuning the temperature, for example [2], or by increasing the volume fraction of the dispersed phase [3] while stirring. Shear-induced phase inversion may be used in industrial processes [4] as it is a way for emulsifying highly viscous liquids like bitumen, for example [5]. Although the inversion phenomenon has been the subject of considerable investigations, the underlying physical mechanisms are still unclear. The sudden feature is one of the most puzzling aspects of such a transition. This situation is partly due to the lack of experimental tools that can probe the *in situ* destabilization processes, in spite of one attempt based on fluorescence techniques [6].

In a recent Letter [7], we have shown that the separation of two neighboring emulsion drops favors their coalescence. Indeed, the separation leads to a pressure reduction in the interstitial film between the two drops that induces a bulging out of the interfaces [8–10]. Therefore, the two interfaces get locally closer, allowing coalescence to be nucleated. We have also demonstrated that such separation-induced coalescence is then responsible of the propagation of coalescence among a compact one-dimensional emulsion. In that case, the shape relaxation during coalescence spontaneously results in a separation with the neighboring drops, a situation that is potentially destabilizing. In this Letter, we again take advantage of the microfluidic tool to follow the destabilization dynamics of a two-dimensional emulsion at the scale of a drop size. A key feature of our system is to

uncouple the formation and the destruction steps of the emulsion. Moreover, the dimensionality of the system offers the possibility to observe new phenomena since it is a step towards the more complex three-dimensional case. Indeed, for the first time, we discover a new mechanism of phase inversion induced by the propagation of drop coalescence. We demonstrate that the probability that neighboring drops merge is a function of their spatial distribution. Then, we discuss the efficiency of this novel scenario of phase inversion. Interestingly, the probability that phase inversion occurs is predicted to be favored by the existence of a drop size distribution.

The details of the fabrication techniques of the microfluidic devices made in poly(dimethylsiloxane) have been previously reported [7]. The dispersed phase is Milli-Q water, and hexadecane is used as the continuous oil phase in which a nonionic surfactant, Span 80, is added. The main part of the device is shown in Fig. 1. We see the formation of a regular and monodisperse train of water-in-oil drops followed by a compaction step of the emulsion obtained by removing part of the oil phase [Fig. 1(a)]. The concentrated emulsion then flows into a chamber having a width of 700  $\mu\text{m}$  and an average height of 27  $\mu\text{m}$ . The converging end of the chamber induces an acceleration of the drops and therefore a separation between neighboring drops. This separation can trigger a first coalescence event that leads to its partial destruction [Fig. 1(b)]. The flow,

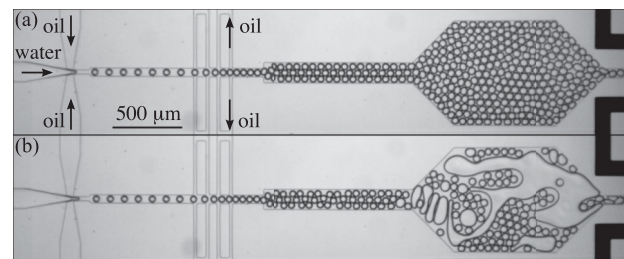


FIG. 1. Fabrication (a) and destruction (b) of a concentrated two-dimensional emulsion in a microfluidic device.

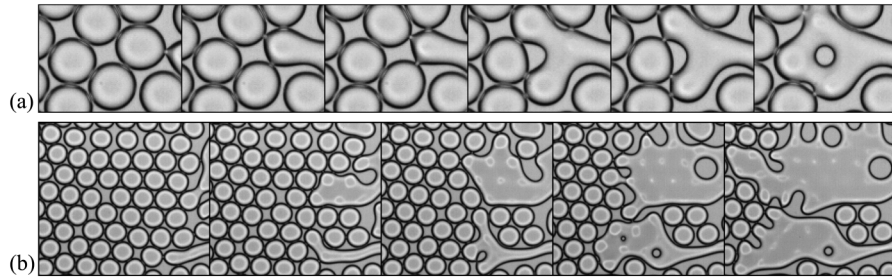


FIG. 2. (a) Time sequence showing a close view of the propagation of drop coalescence that leads to a local phase inversion of the emulsion. The mean drop radius  $R$  is  $20 \mu\text{m}$ , and the time step  $T$  is  $0.133 \text{ ms}$ . (b) Time sequence showing how the coalescence propagates among a concentrated two-dimensional emulsion;  $R = 30 \mu\text{m}$  and  $T = 1.6 \text{ ms}$ .

induced by the chamber geometry, can in a sense be assimilated to the shear of a macroscopic emulsion. In order to prevent coalescence during the compaction step, we add 0.3% in mass of surfactant.

Let us first visualize the propagation of drop coalescence among the two-dimensional emulsion. The image sequence reported in Fig. 2(a) shows a close view of the emulsion destabilization. We clearly observe the driving mechanism of the propagation: The shape relaxation during the merging of two drops induces a separation with the neighboring drops that triggers coalescence. More importantly, we observe the entrapment of the continuous phase via the fusion of a quadruplet of drops that seem to be in contact. This phenomenon can be assimilated to a two-dimensional phase inversion. In the experiment shown in Fig. 2(a), the time interval  $\Delta t_c$  between two successive coalescence events is about  $0.3 \text{ ms}$ . The drop radius  $R$  being  $20 \mu\text{m}$ , we can estimate a velocity of propagation  $U_c$  of the coalescence to be  $U_c = 2R/\Delta t_c \sim 0.13 \text{ m/s}$ . Therefore, the same emulsion contained in a beaker having a size of  $10 \text{ cm}$  would collapse in less than  $1 \text{ s}$ . A larger view of the propagation is reported in Fig. 2(b). In that case,  $\Delta t_c$  is of the order of  $0.6 \text{ ms}$  and  $R$  is equal to  $30 \mu\text{m}$ , leading to  $U_c$  close to  $0.10 \text{ m/s}$ . A smaller drop size seems to lead to a faster propagation. We also note the concomitance of several phase inversion events along with phase separation. The aforementioned features of the propagation of drop coalescence are now discussed in more detail.

The propagation is driven by the shape relaxation of coalescing drops due to the interfacial tension between the two liquids. We therefore focus on the coalescence dynamics of two isolated drops as reported in Fig. 3(a). The generation of a highly diluted emulsion, that flows through the microfluidic chamber shown in Fig. 1, allows us to monitor isolated coalescence events. Indeed, drop pairs are erratically formed, and their coalescence is triggered when the flow moves them apart. The temporal evolution of the distance  $x$  traveled by one pole of the drop during merging and normalized by the maximal displacement  $x_m$  is reported in Fig. 3(b). The relaxation dynamics is well described by the motion of an overdamped oscillator:  $x/x_m = 1 - \exp(-t/\tau)$ ,

where  $\tau$  represents the characteristic time of the damping due to viscous dissipation. The damping time  $\tau$  increases with the drop radius  $R$ , as shown in Fig. 3(c) (●). Moreover,  $\tau$  seems to follow an exponential growth with  $R$  or close to a power law  $\tau \sim R^{6.5}$ . The strong augmentation of the viscous dissipation is a hydrodynamical signature of the vertical confinement since a  $R^{-2}$  dependence is expected for the damping rate of an isolated oscillating drop [11]. The time interval  $\Delta t_c$  between two successive coalescence events is reported in Fig. 3(c) (■). We also note that  $\Delta t_c$  is an increasing function of  $R$  but with a much weaker dependence close to a linear relationship. This last observation clearly indicates that the local dynamics inside the interstitial film plays an important role in the whole propagation dynamics. The resulting velocity of coalescence propagation  $U_c$  lies between  $7$  and  $20 \text{ cm/s}$  for the present formulation and is a decreasing function of the drop size.

The motion of the coalescence front can thus be linked to a relaxation process during coalescence of neighboring

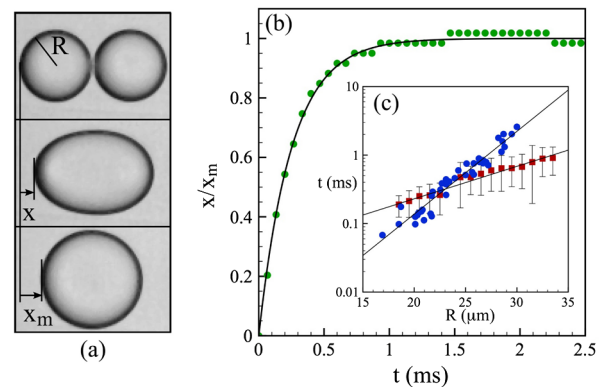


FIG. 3 (color online). (a) Coalescence of two isolated drops with  $R = 22 \mu\text{m}$ . (b) Temporal evolution of the distance  $x$  traveled by one pole of the drop normalized by the maximal displacement  $x_m$ . The symbols are experimental data from (a), and the continuous line represents an exponential fit. (c) Relaxation time  $\tau$  (●) and time interval  $\Delta t_c$  between two successive coalescence events (■) as a function of the drop radius.

drops. Knowing that the coalescence of two drops leads to a nonisotropic flow [12], we wonder how this characteristic does impact on the propagation features. More importantly, what are the required conditions that lead to phase inversion via this autocatalyticlike mechanism? We therefore evaluate the probability  $P_c$  that a merging drop pair induces the coalescence of a neighboring drop as a function of the angle  $\theta$  between the drops. This probability, reported in Fig. 4(a), is constructed as follows: Each time a coalescence event occurs, all the neighboring drops that are apparently in contact, i.e., for which we do not detect an oil film between them, and make an angle  $\theta$  with the drops that have just fused are stored. The conditional probability  $P_c$  is then calculated by dividing the number of the angles  $\theta$  that lead to coalescence by the number of all the angles encountered during many propagation events [Fig. 4(b)]. We did not observe any drastic influence of the drop size  $R$  on the shape of  $P_c$ , which is then evaluated for various drop sizes and volume fractions. The probability is deduced from 2622 coalescence events over 7270 probed drops and includes all the drop sizes reported in Fig. 3(c). The coalescence probability is maximum for aligned drops and then decreases to zero for angles larger than  $130^\circ$ . This azimuthal dependence is a manifestation of the flow induced by the coalescence phase of two drops that exhibits a maximum inward velocity, and thus a large separation rate, for small angles [12].

After having evaluated the probability of coalescence  $P_c(\theta)$ , we wonder how this azimuthal dependence does impact on the emulsion features that is left being the passage of the coalescence front. More precisely, we would like to estimate the probability  $P_i$  that the coalescence propagation results in the entrapment of the continuous phase, namely, to phase inversion. For a two-dimensional case, inversion requires a minimum of three drops in

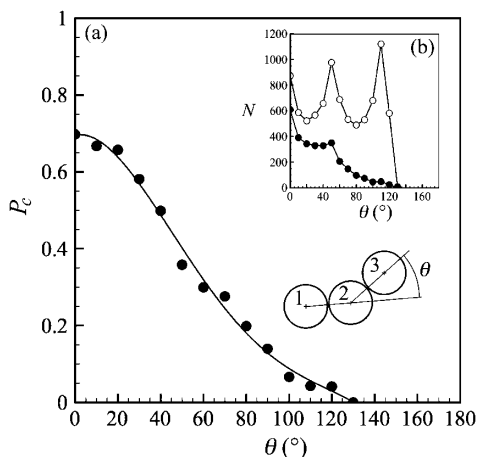


FIG. 4. (a) Probability of coalescence  $P_c$  during the propagation as a function of the angle  $\theta$  between the drops. The continuous line is a fourth-order polynomial fit. (b) Number of the angles  $\theta$  that lead to coalescence (●) among the angles encountered during many coalescence propagations (○).

contact. Unfortunately, this configuration leads to a weak probability for inversion since a large angle comes into play, equal to  $120^\circ$  for monodisperse drops, that results in  $P_i \sim 1\%$  (see below for more details). A more favorable situation for inversion implies four drops as observed in Fig. 2(a). Let us evaluate  $P_i$  starting with drops of equal size  $R$ . As sketched in Fig. 5(a), two angles  $\theta_1$  and  $\theta_2 = 2\theta_1$  are involved in the quadruplet geometry that depend on the diagonal  $D$  of the quadruplet:  $\cos\theta_1 = D/4R$ . The probability that phase inversion occurs is the product of the probabilities that the drop pair (1, 2) coalesces and leads to the fusion of pair (2, 3) and that the pair (1, 4) coalesces and leads to the fusion of pair (4, 3), i.e.,  $P_i = [P_c(\theta_1) \times P_c(\theta_2)]^2$ . The probability  $P_i$  is calculated from a fourth-order polynomial fit of  $P_c$  [Fig. 4(a)] and reported in Fig. 5(a) as a function of  $D/R$ . For clarity, the direction defined by the initial direction of the propagation is aligned along the quadruplet's diagonal.  $P_i$  increases with  $D$  and is maximum for a close-packed situation for which the average direction of propagation is aligned along the crystal axis that minimizes the angles between the drops. Since usual emulsions are characterized by a drop size distribution, we then discuss the effect of drop size variability on the inversion efficiency. To simplify the discussion, we consider a bimodal distribution with a drop size ratio equal to  $\alpha$  and a symmetrical quadruplet [see Fig. 5(a)]. The probability  $P_i$  to inverse is evaluated for  $\alpha = 0.5$  and is reported in Fig. 5(a) as a function of  $D/R$ . We observe a higher probability that a local phase inversion event occurs than for a monodisperse situation.

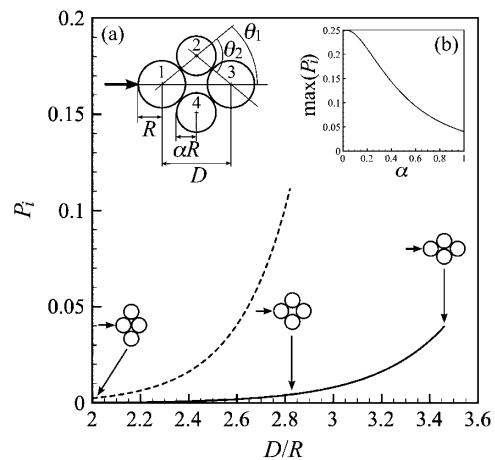


FIG. 5. (a) Probability  $P_i$  that phase inversion occurs via the coalescence of four drops having radii  $R$  and  $\alpha R$  as a function of the distance  $D$  between the two largest drops for  $\alpha = 1$  (straight line) and  $\alpha = 0.5$  (dashed line). This theoretical probability is deduced from the probability of coalescence  $P_c$  which is a function of the angles  $\theta_1$  and  $\theta_2$ , i.e.,  $P_i = [P_c(\theta_1) \times P_c(\theta_2)]^2$  (see more details in the text). Note that the direction of the initial coalescence front is indicated by a horizontal arrow. (b) Maximum probability of phase inversion as a function of the drop size ratio  $\alpha$ .



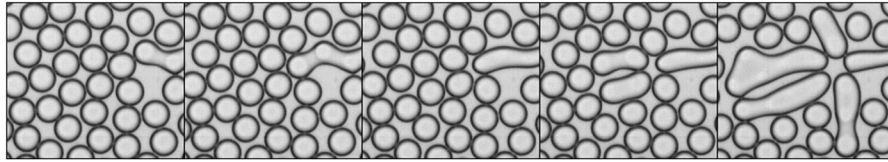


FIG. 6. Time sequence showing that the shape relaxation of the interface after coalescence can indirectly trigger coalescence of far away neighboring drops. The propagation of coalescence can thus be reinitiated. The mean drop radius is  $23 \mu\text{m}$ , and the acquisition time is 0, 0.07, 0.6, 1, and 1.87 ms from left to right.

Moreover, the maximum of  $P_i$  is a decreasing function of  $\alpha$  [Fig. 5(b)]. Therefore, it is expected that the polydispersity feature of an emulsion favors its phase inversion.

Up to now, we have considered only the coalescence of the closest neighboring drops. In reality, coalescence can be initiated two drops away from a coalescence location if a nearby coalescence fails as reported in Fig. 6. Indeed, the motion of the neighboring drops induced by the shape relaxation of a coalescence finger can lead to the fusion of these drops with their closest neighbors. Thus, the avalanche of coalescence can be reinitiated. We note that a similar phenomenon of coalescence induced by coalescence has been previously reported in diluted emulsions [13–15]. In that case, the discussion was focused on the collision between drops which is engendered by the flow generated during the merging phase. However, a clear description of the drop motion induced by the interface relaxation during coalescence within a concentrated emulsion is still lacking. The anisotropic feature of such a flow is shown to be directly connected to a probability of coalescence that indeed depends on the azimuthal distribution of the drops. We point out that this probability incorporates any variations of the interstitial film thickness between adjacent drops. This information is not accessible with the present experimental setup and may define the absolute value of the probability for coalescence like in collapsing foams during avalanches of popping bubbles [16–18]. Moreover, in bulk experiments phase inversion is obtained by continuous shearing, while in our experiments a local shear is induced by a constriction of the microfluidic chamber. Therefore, for bulk experiment situations, many propagation events are expected to occur that will interact and may increase the number of local phase inversion events.

For the first time, we report a dynamic process that leads to the phase inversion of an emulsion. The underlying mechanism relies on the coalescent nature of drop coalescence which can then propagate in a concentrated emulsion. This process is expected to be favored by the existence of a drop size distribution. The present experimental approach, based on microfluidic techniques, has allowed us to probe the destabilization dynamics of a two-dimensional emulsion and thus to follow the intrinsic physical processes at the drop level. A natural extension to

this work would be to investigate such propagation of drop coalescence in more complex situations, like in a three-dimensional emulsion, but new and innovative experimental strategies are still needed.

We acknowledge Howard Stone for stimulating discussions and Denis Bartolo for his careful reading of the manuscript.

\*Nicolas.Bremond@espci.fr

- [1] J. Bibette, F. L. Calderon, and P. Poulin, *Rep. Prog. Phys.* **62**, 969 (1999).
- [2] K. Shinoda and H. Saito, *J. Colloid Interface Sci.* **26**, 70 (1968).
- [3] B. W. Brooks and H. N. Richmond, *Chem. Eng. Sci.* **49**, 1065 (1994).
- [4] J.-L. Salager, A. Forgari, L. Marquez, A. Pena, A. Pizzino, M. P. Rodriguez, and M. Rondon-Gonzalez, *Adv. Colloid Interface Sci.* **108–109**, 259 (2004).
- [5] F. Leal-Calderon, V. Schmitt, and J. Bibette, *Emulsion Science—Basic Principles* (Springer, New York, 2007).
- [6] L. Liu, O. K. Matar, E. S. Perez de Ortiz, and G. F. Hewitt, *Chem. Eng. Sci.* **60**, 85 (2005).
- [7] N. Bremond, A. R. Thiam, and J. Bibette, *Phys. Rev. Lett.* **100**, 024501 (2008).
- [8] L. G. Leal, *Phys. Fluids* **16**, 1833 (2004).
- [9] A. Lai, N. Bremond, and H. A. Stone, *J. Fluid Mech.* **632**, 97 (2009).
- [10] D. Y. C. Chan, E. Klaseboer, and R. Manica, *Soft Matter* **5**, 2858 (2009).
- [11] C. A. Miller and L. E. Scriven, *J. Fluid Mech.* **32**, 417 (1968).
- [12] J. Eggers, J. R. Lister, and H. A. Stone, *J. Fluid Mech.* **401**, 293 (1999).
- [13] H. Tanaka, *Phys. Rev. Lett.* **72**, 1702 (1994).
- [14] V. S. Nikolayev, D. Beysens, and P. Guenoun, *Phys. Rev. Lett.* **76**, 3144 (1996).
- [15] K. S. McGuire, A. Laxminarayan, D. S. Martula, and D. R. Lloyd, *J. Colloid Interface Sci.* **182**, 46 (1996).
- [16] W. Muller and J. M. di Meglio, *J. Phys. Condens. Matter* **11**, L209 (1999).
- [17] N. Vandewalle and J. F. Lentz, *Phys. Rev. E* **64**, 021507 (2001).
- [18] H. Ritacco, F. Kiefer, and D. Langevin, *Phys. Rev. Lett.* **98**, 244501 (2007).